

# Regularizing thermo and magnetic contributions within non renormalizable theories

Sidney S. Avancini,<sup>1,\*</sup> Ricardo L. S. Farias,<sup>2,†</sup> Marcus B. Pinto,<sup>1,‡</sup> Túlio E. Restrepo,<sup>1,3,§</sup> and William R. Tavares<sup>1,¶</sup>

<sup>1</sup>*Departamento de Física, Universidade Federal de Santa Catarina, Florianópolis, SC 88040-900, Brazil*

<sup>2</sup>*Departamento de Física, Universidade Federal de Santa Maria, Santa Maria, RS 97105-900, Brazil*

<sup>3</sup>*CFisUC - Center for Physics of the University of Coimbra,  
Department of Physics, Faculty of Sciences and Technology,  
University of Coimbra, 3004-516 Coimbra, Portugal*

We discuss the importance of implementing a proper regularization procedure in order to treat thermo and magnetic contributions within non renormalizable theories so that physically meaningful results can be obtained. Our investigation suggests that potential divergences should be first completely isolated into the vacuum and purely magnetic contributions which are then regularized while the convergent thermomagnetic contributions should be integrated over the full momentum range without any regulators. The procedure is illustrated by applying the proper time formalism to the two flavor Polyakov–Nambu–Jona-Lasinio model, whose magnetic field dependent coupling has been recently determined. Observables such as the pressure, magnetization, speed of sound squared, and the specific heat evaluated with the proposed prescription are compared with results furnished by other three possible regularization prescriptions which are often adopted in the literature. It turns out that, when evaluated with our method, these quantities display thermomagnetic behaviors which are physically more consistent than the ones predicted with other regularization schemes. In particular, we demonstrate that naively regulating the (entangled) vacuum, magnetic and thermomagnetic contributions leads to physically inconsistent results especially at the high temperature domain.

---

\* [sidney.avancini@ufsc.br](mailto:sidney.avancini@ufsc.br)

† [ricardo.farias@uol.com.br](mailto:ricardo.farias@uol.com.br)

‡ [marcus.benghi@ufsc.br](mailto:marcus.benghi@ufsc.br)

§ [tulio.restrepo@posgrad.ufsc.br](mailto:tulio.restrepo@posgrad.ufsc.br)

¶ [william.tavares@posgrad.ufsc.br](mailto:william.tavares@posgrad.ufsc.br)

## I. INTRODUCTION

Understanding the behavior of magnetized quark matter is of fundamental importance for the correct description of physical situations that may take place in magnetars as well as in peripheral heavy ion collisions [1–4]. On the theoretical side this problem has received a lot of attention recently through the use lattice QCD (LQCD) numerical simulations and analytical model approximations. One controversy has emerged when precise LQCD applications, carried out at zero baryonic densities and physical pionic masses, have indicated that the cross over pseudocritical temperature ( $T_{pc}$ ) should decrease with increasing magnetic field values [5, 6]. This outcome contradicts early LQCD simulations [7–9], where high pionic mass values were considered<sup>1</sup>, and also analytical evaluations (mostly at the mean field level) performed with effective theories such as the ones described by the Nambu–Jona-Lasinio model (NJL) [11] and the quark meson model (QMM) [12, 13] as well as their Polyakov loop extended versions (PNJL [14] and PQMM [15] respectively). The possible origin of this discrepancy has later been elucidated in Ref. [16] where the authors have shown that adding pionic loops to the mean field quark pressure could fix the problem. Another possible alternative is to include thermo-magnetic effects on the coupling constants [17–23]. This approach has been adopted in various investigations where different possible *ansatz* [24–27] to describe the  $B$ -dependent running of the coupling have been proposed leading to results for  $T_{pc}$  which are in line with LQCD predictions. The same type of technique has been generalized to the SU(3) PNJL model where the six fermion coupling has also been fixed according to LQCD data [28]. The reader is referred to Ref. [29] for a comprehensive review on effective models under strong magnetic fields

More recently the two-flavor PNJL model coupling has been fixed by using, as input, LQCD results that determine the baryon spectrum of 1+1+1-flavors in the presence of a strong magnetic background and at physical pionic masses [25]. In this case the model running coupling,  $G(B)$ , has been determined by constraining the PNJL constituent quark mass to match the LQCD results including, of course, the decrease of  $T_{pc}$  with  $B$ . For the present work it is important to remark that to evaluate quantities such as the pressure the authors of Ref. [25] have adopted Schwinger’s proper time formalism [30] and regularized *all* integrals without separating the divergent (vacuum) piece from the convergent (thermomagnetic) contribution. Next, this regularization choice has been used to evaluate the effective mass, the quark condensate, and the pressure for  $eB = 0$  to  $0.6$  GeV<sup>2</sup> covering temperatures up to  $T \approx 0.27$  GeV so that the final result for  $T_{pc}(B)$  is in good agreement with LQCD predictions. Nevertheless, it is now well established that such a regularization procedure can give rise to a series of inconsistencies if the calculations are pushed to higher temperatures (when, e.g., the pressure may not converge to the Stefan-Boltzmann limit, as observed in the case  $eB = 0$  [31–33]) or to finite baryon chemical potentials (where the appearance of unphysical oscillations is more noticeable). For example, using a  $B$ -dependent regularization scheme for the calculation of the magnetization some authors find oscillations which are unphysical while others find imaginary meson masses which are in fact spurious solutions due to the inappropriate choice of the regularization. This can be seen by comparing the meson masses results of Ref. [34] where real values can only be reproduced upon implementing a consistent regularization strategy. The importance of using an appropriate regularization scheme to describe magnetized quark matter has been clearly demonstrated in Refs. [35, 36] which suggest a strong dependence on the choice of the regularization scheme for the calculation of physical observables and, more importantly, that an inappropriate regularization scheme may give rise to spurious solutions. Here, our main goal is to investigate different regularization schemes in order to select the ones which produce physically more reliable results as far as non renormalizable theories are concerned. With this aim it is important to first recall the possibility that different regularization (and renormalization) procedures implemented to treat divergences in quantum field theories always introduce some degree of arbitrariness during formal evaluations. Generally, within renormalizable theories such as QCD this arbitrariness is associated to the possibility of choosing different regulators, subtraction points, and energy scales. However, physically unambiguous results may be obtained by further constraints such as the ones imposed by the renormalization group equations which require that physical observables be invariant with respect to changes in arbitrary energy scale. The situation is less clear when it comes to non renormalizable theories such as the PNJL model in  $3 + 1d$  considered here. Traditionally, this type of theory is regularized with a sharp cut-off<sup>2</sup>,  $\Lambda$ , which instead of being removed by some subtraction prescription is formally treated as a “parameter” that sets the scale value (generally  $\sim 0.6 – 1$  GeV) up to which the theory can be considered to be effective [38]. In the absence of control parameters such as  $T$ ,  $\mu$ , and  $B$ , where it is free from ambiguities, this became the standard procedure to deal with NJL type of models. The case of  $T = B = 0$  and  $\mu \neq 0$  is also unambiguous since the Fermi momentum,  $p_F = (\mu^2 - M^2)^{1/2}$ , naturally regularizes the convergent contributions. When finite temperatures come into play (still at  $B = 0$ ) the thermodynamical potential at the (one loop) mean field level considered here split into two parts  $\Omega = \Omega_V + \Omega_T$  where the first represents the ultra violet (UV) divergent vacuum piece and the second one represents the convergent thermal contribution. In renormalizable theories one

<sup>1</sup> In a recent LQCD study [10], the authors obtain the decrease of  $T_{pc}$  with increasing magnetic fields when heavy pions are considered.

<sup>2</sup> See Ref. [37] for alternatives such as dimensional regularization.

usually isolates and renormalizes the divergences contained in  $\Omega_V$  so that its final contribution is finite in the extreme UV limit and does not depend on any regulator. At the same time the convergent thermal integrals are simply integrated over the full momentum range. When considering non renormalizable theories where the final vacuum contribution depends on the regulator (now a finite valued “parameter”) one has two options to treat the thermal part. In early works (see Ref. [39] and references therein) the preferred method was that (for “consistency”) one should also regularize the convergent thermal integrals so that  $\Omega = \Omega_V(\Lambda) + \Omega_T(\Lambda)$ . More recently it has been suggested that this course of action is unnecessary since the finite temperature contribution has a natural cut-off in itself specified by the temperature [40] and in this case one should consider  $\Omega = \Omega_V(\Lambda) + \Omega_T(\infty)$  where in the second term the symbol  $\infty$  is a reminder that this finite contribution has not been regularized (that is,  $\Lambda \rightarrow \infty$ ). The drawback associated with the former approach is that thermodynamical quantities evaluated in this way do not converge to the expected Stefan-Boltzmann limit as  $T \rightarrow \infty$  [39]. On the other hand, although the latter strategy does not spoil the high- $T$  behavior of quantities such as the pressure it can generate thermal effective masses which are smaller than the actual current mass value,  $m_c$ , which is also undesirable [33] although, in general, this happens at temperatures of the order  $T \approx M(0)$  where  $M(0)$  represents the effective quark mass at zero temperature,  $M(0) \approx 300$  MeV. It should be mentioned that alternatives to recover the Stefan-Boltzmann limit while maintaining  $M(T) > m_c$  at high- $T$  have been given in Ref. [41, 42].

Additional care is needed when regularizing a non renormalizable theory to describe magnetized hadronic matter since in this case the vacuum energy acquires a Landau level (LL) structure. In this scenario early works [43], at  $T = 0$ , employed Schwinger’s proper time formalism without disentangling the purely magnetic part from the vacuum so that  $\Omega = \Omega_{VM}(\Lambda)$  meaning that the vacuum and magnetic divergences are entangled and have been regularized (still at  $T = 0$ ). Adding finite temperature effects within this formalism brings in, once again, the question about the need to regularize (or not) the finite thermomagnetic contribution  $\Omega_{TM}$  contained in  $\Omega$ . Since these two possibilities will be examined here let us dub standard proper time (SPT) the one in which  $\Omega_{TM}$  is *not* regularized so that  $\Omega = \Omega_{VM}(\Lambda) + \Omega_{TM}(\infty)$  and, at the same time, let us dub thermomagnetic regulated proper time scheme (TRPT) the one in which  $\Omega_{TM}$  is regularized as in Ref. [25] so that  $\Omega = \Omega_{VM}(\Lambda) + \Omega_{TM}(\Lambda)$ . Later, the interesting possibility of isolating all the divergences within the vacuum term by separating a finite purely magnetic term (summed over all Landau levels, LL) has been suggested [44, 45]. This scheme, which avoids unphysical oscillations, was originally applied in the PT framework [45] and latter generalized to the sharp cutoff framework [46] allowing for several further applications [36, 47–54]. Within this magnetic field *independent* regularization scheme<sup>3</sup> (MFIR), which uses dimensional regularization techniques, a magnetic field dependent divergence is *subtracted* together with other finite mass independent ( $B$ -dependent) terms so that, at  $T = 0$ , one ends up with  $\Omega = \Omega_V(\Lambda) + \Omega_M$  where  $\Omega_M$  represents a purely magnetic finite contribution that does not require further integration or sum over LL. As before, when going to finite temperatures one needs to add the thermomagnetic contribution  $\Omega_{TM}(\Lambda)$  or  $\Omega_{TM}(\infty)$  to  $\Omega$  (here we will consider the latter case which is the one most adopted in the literature). At this point it is legitimate to ask how the MFIR subtraction prescription may affect physical observables since subtracting mass independent terms means that finite  $B$ -dependent terms also end up by being neglected. One may argue that adopting this scheme to analyze phase transitions as in Refs. [44, 46] through order parameters such as the quark condensate,  $\langle \bar{\psi} \psi \rangle = \partial \Omega / \partial m_c$ , can be justified because these quantities are mass dependent. However, this scheme may not be appropriate to treat other quantities such as the magnetization,  $\mathcal{M} = -\partial \Omega / \partial B$ , since one needs the *complete*  $\Omega$  including all finite  $B$ -dependent terms (see Ref. [55] for a related discussion). In order to circumvent this eventual problem a fourth possibility which avoids any subtractions will be proposed in the present work. Within this prescription one starts by isolating the purely magnetic part of  $\Omega$  and then identifying two potential divergences: one which is  $B$ -independent ( $M$ -dependent) and another one which is  $B$ -dependent ( $M$ -independent) just as in the MFIR case. However, the most important difference is that now the  $B$ -dependent divergence is simply regularized but not subtracted (by renormalizing  $(eB)^2$ ) as in the MFIR case so that, at  $T = 0$ , the thermodynamical potential has the form  $\Omega = \Omega_V(\Lambda) + \Omega_M(\Lambda)$  (when considering the  $T \neq 0$  case in this scheme we will consider a non regularized piece,  $\Omega_{TM}(\infty)$ ). We shall dub this prescription vacuum magnetic regularization scheme (VMR) since the divergences present in the vacuum and purely magnetic contributions are regulated. In summary, the fact that at  $B \neq 0$  the lagrangian density of non renormalizable models is enlarged by a *finite* QED type of sector together with the additional possible choices of regularizing the convergent thermomagnetic generates a great number of possible regularization prescriptions. Unfortunately, dealing with divergences in non renormalizable theories in the presence of a magnetic field and a thermal bath cannot be dealt with in a pragmatic manner as in the case of renormalizable theories where, as already discussed, further constraints based on a well established renormalization programme are available. Nevertheless, one may analyze the physical behavior of different observables as a guide to select the most appropriate regularization prescription to investigate hot magnetized strongly interacting matter when it is described by a non renormalizable theory. With this purpose in

<sup>3</sup> More recently the MFIR has been further improved by means of the Hurwitz-Riemann zeta function defining the so called zeta MFIR (zMFIR) regularization procedure [51].

this work we will consider the four possible regularization schemes already described to evaluate physical quantities such as the quark condensate, pressure, magnetization, speed of sound, and specific heat at finite temperatures and in the presence of a strong magnetic field. The work is organized as follows. In the next section we present the model and review finite temperature results in the absence of magnetic fields. Then, in Sec.III, we obtain the thermodynamical potential using four possible regularization prescriptions. Numerical results are presented in Sec. IV and the conclusions in Sec. V.

## II. THE MODEL

The PNJL Lagrangian density in the presence of an external magnetic field is given by [40]

$$\mathcal{L}_{PNJL} = \bar{\psi} (i\gamma_\mu D^\mu - \hat{m}_c) \psi + G \left[ (\bar{\psi}\psi)^2 + (\bar{\psi}i\gamma_5 \tau\psi)^2 \right] - \mathcal{U}(\Phi, \bar{\Phi}, T) - \frac{1}{4} F^{\mu\nu} F_{\mu\nu}, \quad (2.1)$$

where  $\psi$  represents fermionic fields (a sum in color and flavor indices is implicit),  $\tau$  are isospin Pauli matrices,  $\hat{m}_c$  are the current quark masses which, for simplicity, we set as  $m_u = m_d \equiv m_c$  while  $G$  represents the coupling constant. The covariant derivative is given by

$$D^\mu = \partial^\mu - iq_f A_{EM}^\mu - iA^\mu, \quad (2.2)$$

where  $q_f$  represents the quark electric charge<sup>4</sup>,  $A_{EM}^\mu$  is the electromagnetic gauge field,  $F^{\mu\nu} = \partial^\mu A_{EM}^\nu - \partial^\nu A_{EM}^\mu$  where  $A_{EM}^\mu = \delta_{\mu 2} x_1 B$  and  $\vec{B} = B \hat{e}_3$  within the Landau gauge adopted here. We also consider the Polyakov gauge where the gluonic term,  $A^\mu = g A_a^\mu(x) \frac{\lambda_a}{2}$ , only contributes with the spatial components:  $A^\mu = \delta_\mu^0 A^0 = -i\delta_\mu^0 A^4$  where  $g$  is the strong coupling,  $A_a^\mu(x)$  represents the SU(3) gauge fields while  $\lambda_a$  are the Gell-Mann matrices. The expectation value of the Polyakov loop,  $\Phi$ , is then given by the expected value of the Wilson line [56],  $L(\mathbf{x}) \equiv \mathcal{P} \exp \left[ i \int_0^\beta d\tau A_4(\tau, \mathbf{x}) \right]$ . That is,

$$\Phi \equiv \left\langle \frac{1}{N_c} \text{Tr} L(\mathbf{x}) \right\rangle, \quad \text{and} \quad \bar{\Phi} \equiv \left\langle \frac{1}{N_c} \text{Tr} L^\dagger(\mathbf{x}) \right\rangle. \quad (2.3)$$

Remark that the Polyakov potential,  $\mathcal{U}(\Phi, \bar{\Phi}, T)$ , is fixed to reproduce pure-gauge LQCD results [14]. In the case of vanishing baryonic densities ( $\mu = 0$ ) considered here one has  $\bar{\Phi} = \Phi$  so that the ansatz proposed in Ref. [57] reads

$$\frac{\mathcal{U}(\Phi, T)}{T^4} = -\frac{1}{2} b_2(T) \Phi^2 + b_4(T) \ln [1 - 6\Phi^2 + 8\Phi^3 - 3\Phi^4], \quad (2.4)$$

with

$$b_2(T) = a_0 + a_1 \left( \frac{T_0}{T} \right) + a_2 \left( \frac{T_0}{T} \right)^2, \quad b_4(T) = b_4 \left( \frac{T_0}{T} \right)^3, \quad (2.5)$$

where the parametrization is given in table I. Following Ref. [25] we choose  $T_0 = 208$  MeV in order to consider two quark flavor corrections [58].

$a_0$	$a_1$	$a_2$	$b_4$
3.51	-2.47	15.22	-1.75

TABLE I. Parameter set used for the Polyakov loop potential

## III. THERMODYNAMICAL POTENTIAL EVALUATIONS

Let us now evaluate the thermodynamical potential,  $\Omega(M, \Phi, T, B)$ , by applying the MFA to the PNJL within the proper time (PT) framework. As discussed in the introduction the divergences will be handled in four different ways.

<sup>4</sup>  $q_u = 2e/3$ ,  $q_d = -e/3$  with  $e = 1/\sqrt{137}$

### A. TRPT and SPT frameworks

Within the regulated thermomagnetic integral PT formalism (TRPT) adopted in Ref. [25] the thermodynamical potential is

$$\Omega_{TRPT}(M, \Phi, T, B) = \mathcal{U}(\Phi, T) + \frac{(M - m_c)^2}{4G} + \frac{N_c}{8\pi^2} \sum_{f=u,d} |q_f B|^2 \int_{\frac{|q_f B|}{\Lambda^2}}^{\infty} \frac{ds}{s^2} e^{-\frac{M^2 s}{|q_f B|}} \coth(s) + \frac{1}{8\pi^2} \sum_{f=u,d} |q_f B|^2 \int_{\frac{|q_f B|}{\Lambda^2}}^{\infty} \frac{ds}{s^2} e^{-\frac{M^2 s}{|q_f B|}} \coth(s) \left\{ 2 \sum_{n=1}^{\infty} e^{-\frac{|q_f B| n^2}{4sT^2}} (-1)^n \left[ 2 \cos \left( n \cos^{-1} \frac{3\Phi - 1}{2} \right) + 1 \right] \right\}, \quad (3.1)$$

where the effective mass is given by the solution of the self-consistent gap equation

$$\frac{M - m_c}{2G} = \frac{MN_c}{4\pi^2} \sum_{f=u,d} |q_f B| \int_{\frac{|q_f B|}{\Lambda^2}}^{\infty} \frac{ds}{s} e^{-\frac{M^2 s}{|q_f B|}} \coth(s) + \frac{M}{4\pi^2} \sum_{f=u,d} |q_f B| \int_{\frac{|q_f B|}{\Lambda^2}}^{\infty} \frac{ds}{s} e^{-\frac{M^2 s}{|q_f B|}} \coth(s) \left\{ 2 \sum_{n=1}^{\infty} e^{-\frac{|q_f B| n^2}{4sT^2}} (-1)^n \left[ 2 \cos \left( n \cos^{-1} \frac{3\Phi - 1}{2} \right) + 1 \right] \right\}, \quad (3.2)$$

which is to be solved simultaneously with  $\frac{\partial \Omega(M, \Phi, T)}{\partial \Phi}|_{M,T} = 0$ . Remark the presence of the regulator  $|q_f B|/\Lambda^2$  in the lower limit of the *convergent* thermomagnetic integrals represented by the last terms of Eqs. (3.1), and (3.2) which indicates that  $\Omega_{TRPT} = \Omega_{VM}(\Lambda) + \Omega_{TM}(\Lambda)$ . To obtain the equivalent SPT relation one simply needs to consider these convergent terms upon performing the replacement  $|q_f B|/\Lambda^2 \rightarrow 0$  in the lower limit of those integrals so that  $\Omega_{SPT} = \Omega_{VM}(\Lambda) + \Omega_{TM}(\infty)$  as already discussed. For completeness let us also quote the  $B = 0$  relations

$$\Omega_{TRPT}(M, \Phi, T, 0) = \mathcal{U}(\Phi, T) + \frac{(M - m_c)^2}{4G} + \frac{N_c N_f}{8\pi^2} \int_{\frac{1}{\Lambda^2}}^{\infty} \frac{ds}{s^3} e^{-M^2 s} + \frac{N_f}{8\pi^2} \int_{\frac{1}{\Lambda^2}}^{\infty} \frac{ds}{s^3} e^{-M^2 s} \left\{ 2 \sum_{n=1}^{\infty} e^{-\frac{n^2}{4sT^2}} (-1)^n \left[ 2 \cos \left( n \cos^{-1} \frac{3\Phi - 1}{2} \right) + 1 \right] \right\}, \quad (3.3)$$

and

$$\frac{M - m_c}{2G} = \frac{MN_c N_f}{4\pi^2} \int_{\frac{1}{\Lambda^2}}^{\infty} \frac{ds}{s^2} e^{-M^2 s} + \frac{MN_f}{4\pi^2} \int_{\frac{1}{\Lambda^2}}^{\infty} \frac{ds}{s^2} e^{-M^2 s} \left\{ 2 \sum_{n=1}^{\infty} e^{-\frac{n^2}{4sT^2}} (-1)^n \left[ 2 \cos \left( n \cos^{-1} \frac{3\Phi - 1}{2} \right) + 1 \right] \right\}. \quad (3.4)$$

To obtain the equivalent SPT relations one performs the replacement  $1/\Lambda^2 \rightarrow 0$  in the lower limit of the convergent thermal integrals represented by the last terms of Eqs. (3.3) and (3.4).

### B. VMR and MFIR frameworks

The first step to implement the vacuum magnetic regularization scheme proposed here is to split the (divergent) third term of Eq. (3.1) in one  $B$  independent integral and one pure magnetic expression (see Appendix A for details). Then,

$$\frac{N_c}{8\pi^2} \sum_{q_f=u,d} |q_f B|^2 \int_{\frac{|q_f B|}{\Lambda^2}}^{\infty} \frac{ds}{s^2} e^{-\frac{M^2 s}{|q_f B|}} \coth(s) = \frac{N_c N_f}{8\pi^2} \int_{\frac{1}{\Lambda^2}}^{\infty} \frac{ds}{s^3} e^{-M^2 s} + \frac{N_c}{24\pi^2} \sum_{q_f=u,d} |q_f B|^2 \int_{\frac{1}{\Lambda^2}}^{\infty} \frac{ds}{s} e^{-M^2 s} - N_c \sum_{q_f=u,d} \frac{|q_f B|^2}{2\pi^2} \left[ \zeta'(-1, x_f) - [x_f^2 - x_f] \frac{\ln x_f}{2} + \frac{x_f^2}{4} - \frac{1}{12} (1 + \ln x_f) \right], \quad (3.5)$$

where  $x_f = \frac{M}{2|q_f B|}$ , and  $\zeta$  represents the Hurwitz-Riemann zeta function. Up to this point our procedure is similar to the so-called MFIR prescription employed in Ref. [44]. To understand the differences first note that Eq. (3.5) has

two divergences with the first one contained in the vacuum contribution (first term on the rhs) while the second one is contained in the magnetic contribution (second term). Within the MFIR the divergence of the magnetic contribution is completely subtracted by renormalizing  $(eB)^2$  and in this process the finite contributions represented by the terms proportional to  $(1 + \ln x)/12$  are also cancelled so that the purely magnetic contribution is finite. Nevertheless, we advocate that such subtraction, which is implied by the renormalizing the field, should be avoided within non renormalizable theories in order to preserve all  $B$ -dependent terms.

Then, considering Eq. (3.5) together with the finite thermomagnetic contribution one obtains the VMR thermodynamical potential

$$\begin{aligned} \Omega_{VMR}(M, \Phi, T, B) = & \mathcal{U}(\Phi, T) + \frac{(M - m_c)^2}{4G} + \frac{N_c N_f}{8\pi^2} \int_{\frac{1}{\Lambda^2}}^{\infty} \frac{ds}{s^3} e^{-M^2 s} + \frac{N_c}{24\pi^2} \sum_{f=u,d} |q_f B|^2 \int_{\frac{1}{\Lambda^2}}^{\infty} \frac{ds}{s} e^{-M^2 s} \\ & - N_c \sum_{f=u,d} \frac{|q_f B|^2}{2\pi^2} \left[ \zeta'(-1, x_f) - \frac{1}{2} [x_f^2 - x_f] \ln x_f + \frac{x_f^2}{4} - \frac{1}{12} (1 + \ln x_f) \right] \\ & + \frac{1}{8\pi^2} \sum_{f=u,d} |q_f B|^2 \int_0^{\infty} \frac{ds}{s^2} e^{-\frac{M^2 s}{|q_f B|}} \coth(s) \left\{ 2 \sum_{n=1}^{\infty} e^{-\frac{|q_f B| n^2}{4sT^2}} (-1)^n \left[ 2 \cos \left( n \cos^{-1} \frac{3\Phi - 1}{2} \right) + 1 \right] \right\}, \end{aligned} \quad (3.6)$$

which is clearly of the form  $\Omega_{VMR} = \Omega_V(\Lambda) + \Omega_M(\Lambda) + \Omega_{TM}(\infty)$ . Then, the VMR gap equation is given by

$$\begin{aligned} \frac{M - m_c}{2G} = & \frac{MN_c N_f}{4\pi^2} \int_{\frac{1}{\Lambda^2}}^{\infty} \frac{ds}{s^2} e^{-M^2 s} + \frac{MN_c}{12\pi^2} \sum_{f=u,d} |q_f B|^2 \int_{\frac{1}{\Lambda^2}}^{\infty} ds e^{-M^2 s} \\ & + MN_c \sum_{f=u,d} \frac{|q_f B|}{2\pi^2} \left[ \ln(\Gamma[x_f]) - \frac{1}{2} \ln(2\pi) + x_f - \frac{1}{2} (2x_f - 1) \ln x_f - \frac{1}{12x_f} \right] \\ & + \frac{M}{4\pi^2} \sum_{f=u,d} |q_f B| \int_0^{\infty} \frac{ds}{s} e^{-\frac{M^2 s}{|q_f B|}} \coth(s) \left\{ 2 \sum_{n=1}^{\infty} e^{-\frac{|q_f B| n^2}{4sT^2}} (-1)^n \left[ 2 \cos \left( n \cos^{-1} \frac{3\Phi - 1}{2} \right) + 1 \right] \right\}. \end{aligned} \quad (3.7)$$

For completeness let us quote the equivalent MFIR equations [35, 36, 44, 46]

$$\begin{aligned} \Omega_{MFIR}(M, \Phi, T, B) = & \mathcal{U}(\Phi, T) + \frac{(M - m_c)^2}{4G} + \frac{N_c N_f}{8\pi^2} \int_{\frac{1}{\Lambda^2}}^{\infty} \frac{ds}{s^3} e^{-M^2 s} \\ & - N_c \sum_{f=u,d} \frac{|q_f B|^2}{2\pi^2} \left[ \zeta'(-1, x_f) - \frac{1}{2} [x_f^2 - x_f] \ln x_f + \frac{x_f^2}{4} \right] \\ & + \frac{1}{8\pi^2} \sum_{f=u,d} |q_f B|^2 \int_0^{\infty} \frac{ds}{s^2} e^{-\frac{M^2 s}{|q_f B|}} \coth(s) \left\{ 2 \sum_{n=1}^{\infty} e^{-\frac{|q_f B| n^2}{4sT^2}} (-1)^n \left[ 2 \cos \left( n \cos^{-1} \frac{3\Phi - 1}{2} \right) + 1 \right] \right\}, \end{aligned} \quad (3.8)$$

which is of the form  $\Omega_{MFIR} = \Omega_V(\Lambda) + \Omega_M + \Omega_{TM}(\infty)$ . The MFIR gap equation reads

$$\begin{aligned} \frac{M - m_c}{2G} = & \frac{MN_c N_f}{4\pi^2} \int_{\frac{1}{\Lambda^2}}^{\infty} \frac{ds}{s^2} e^{-M^2 s} + MN_c \sum_{f=u,d} \frac{|q_f B|}{2\pi^2} \left[ \ln(\Gamma[x_f]) - \frac{1}{2} \ln(2\pi) + x_f - \frac{1}{2} (2x_f - 1) \ln x_f \right] \\ & + \frac{M}{4\pi^2} \sum_{f=u,d} |q_f B| \int_0^{\infty} \frac{ds}{s} e^{-\frac{M^2 s}{|q_f B|}} \coth(s) \left\{ 2 \sum_{n=1}^{\infty} e^{-\frac{|q_f B| n^2}{4sT^2}} (-1)^n \left[ 2 \cos \left( n \cos^{-1} \frac{3\Phi - 1}{2} \right) + 1 \right] \right\}. \end{aligned} \quad (3.9)$$

#### IV. RESULTS

Having the thermodynamical potential we can easily obtain some important thermodynamical observables such as the pressure,  $P = -\Omega$ , and the energy density,  $\mathcal{E} = -P + T\mathcal{S} + B\mathcal{M}$ , where the entropy density is  $\mathcal{S} = \partial P / \partial T$  and the magnetization is  $\mathcal{M} = \partial P / \partial B$ . For our purposes it will prove useful to also investigate the quark condensate

$$\langle \bar{\psi} \psi \rangle = -\frac{\partial P}{\partial m_c}, \quad (4.1)$$

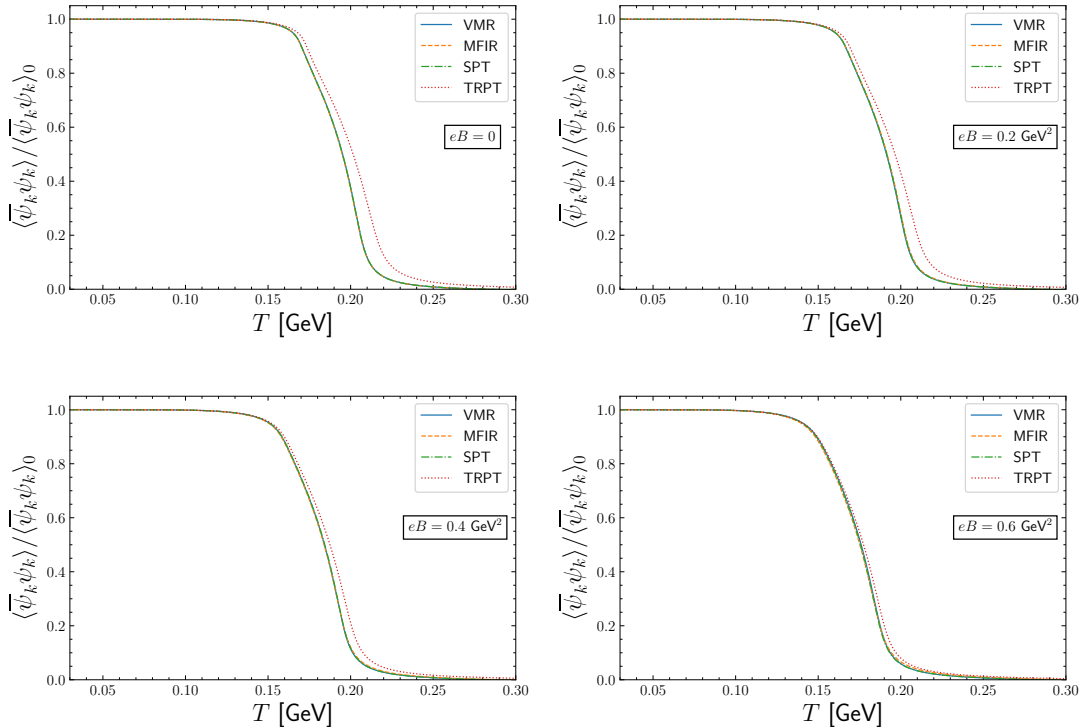


FIG. 1. Normalized quark condensate for different magnetic fields as a function of temperature calculated with the different regularization procedures.

as well as the specific heat and the speed of sound squared which are respectively defined as

$$C_v = T \frac{\partial S}{\partial T}, \quad (4.2)$$

and

$$C_s^2 = \frac{\partial P}{\partial \mathcal{E}} = \frac{S}{C_v}. \quad (4.3)$$

As explained in the introduction, in order to be in line with LQCD predictions we shall consider a  $B$ -dependent coupling,  $G(B)$ , whose running was determined in Ref. [25]. Following that work we first set  $\Lambda = 675$  MeV and  $m_c = 3.5$  MeV and then tune  $G(B)$  so that all four different regularization schemes considered here yield the quark mass value needed to reproduce the mesonic masses predicted by LQCD simulations. The values of the dimensionless quantity  $G(B)\Lambda^2$  at different magnetic intensities are given in table (II) for the four different schemes.

$eB$ [GeV $^2$ ]	VMR	MFIR	SPT and TRPT
0.0	5.83200	5.83200	5.83200
0.2	5.18333	5.05349	5.19413
0.4	4.04762	3.74477	4.05506
0.6	3.07324	2.69719	3.05269

TABLE II.  $G(B)\Lambda^2$  values for the four different regularization prescriptions.

Let us start by analyzing the chiral transition order parameter represented by the quark condensate. Fig. 1 shows this quantity as a function of the temperature for different values of the magnetic field illustrating that except for the TRPT all other regularization schemes predict a similar quantitative behavior. As  $B$  increases the TRPT

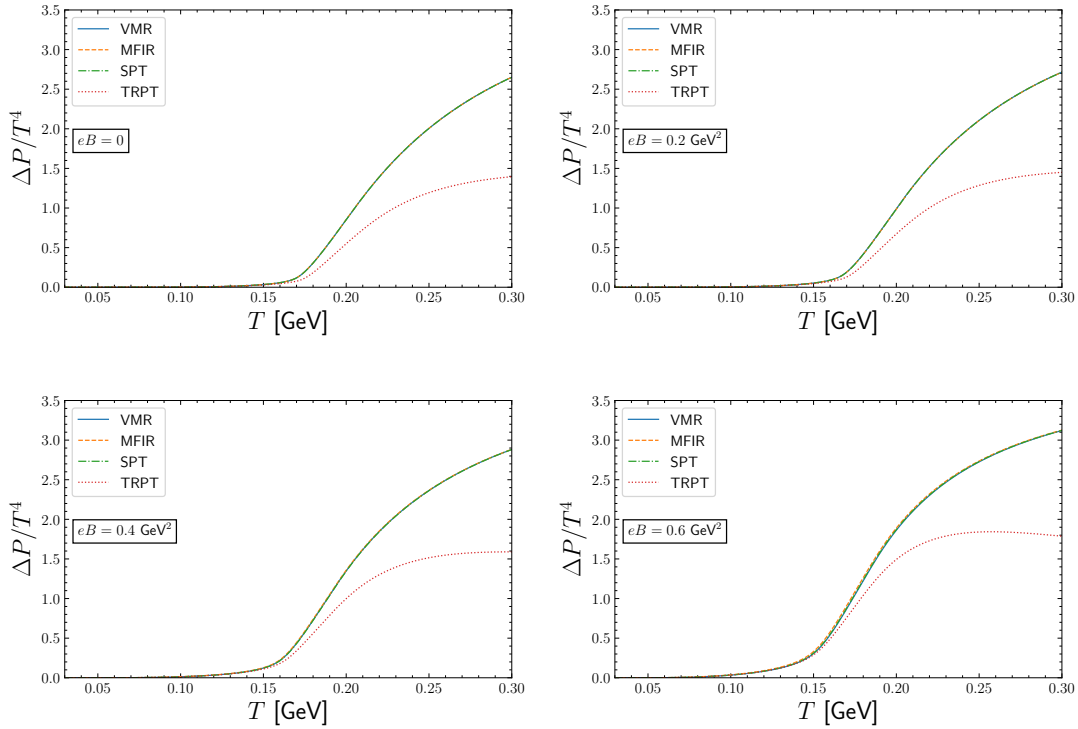


FIG. 2. Normalized pressure for different magnetic field values as a function of temperature calculated with the different regularization procedures.

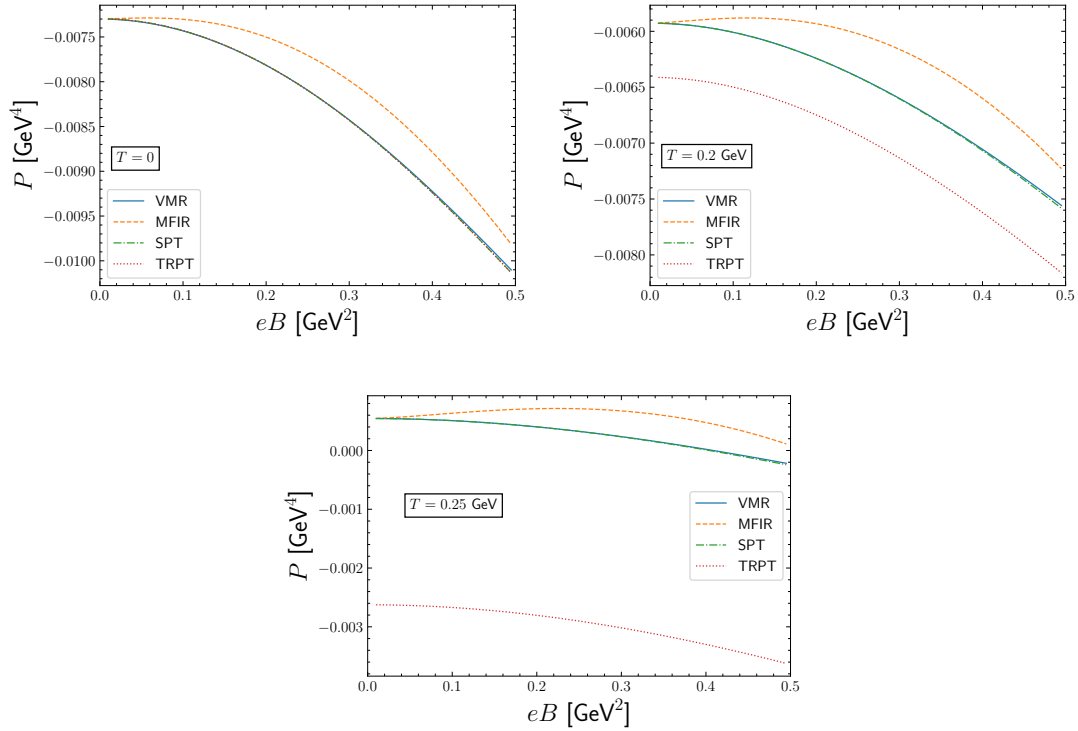


FIG. 3. Pressure for different temperature values as a function of  $eB$  calculated with the different regularization procedures.

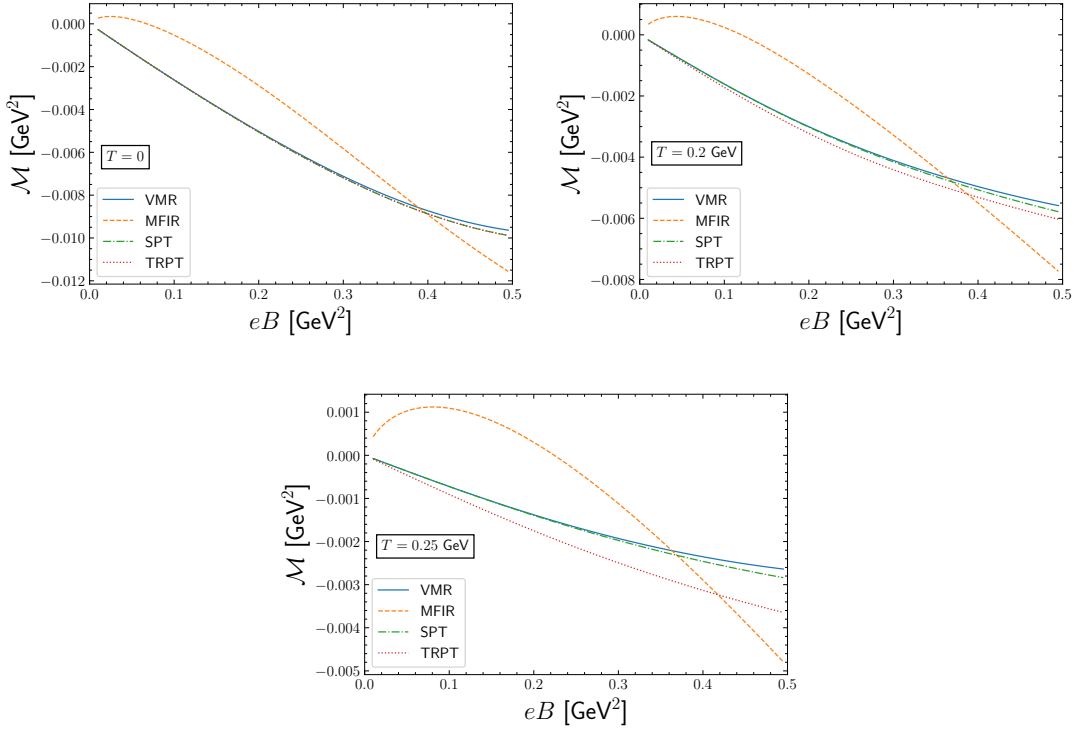


FIG. 4. Magnetization for different temperature values as a function of  $eB$  calculated with the different regularization procedures.

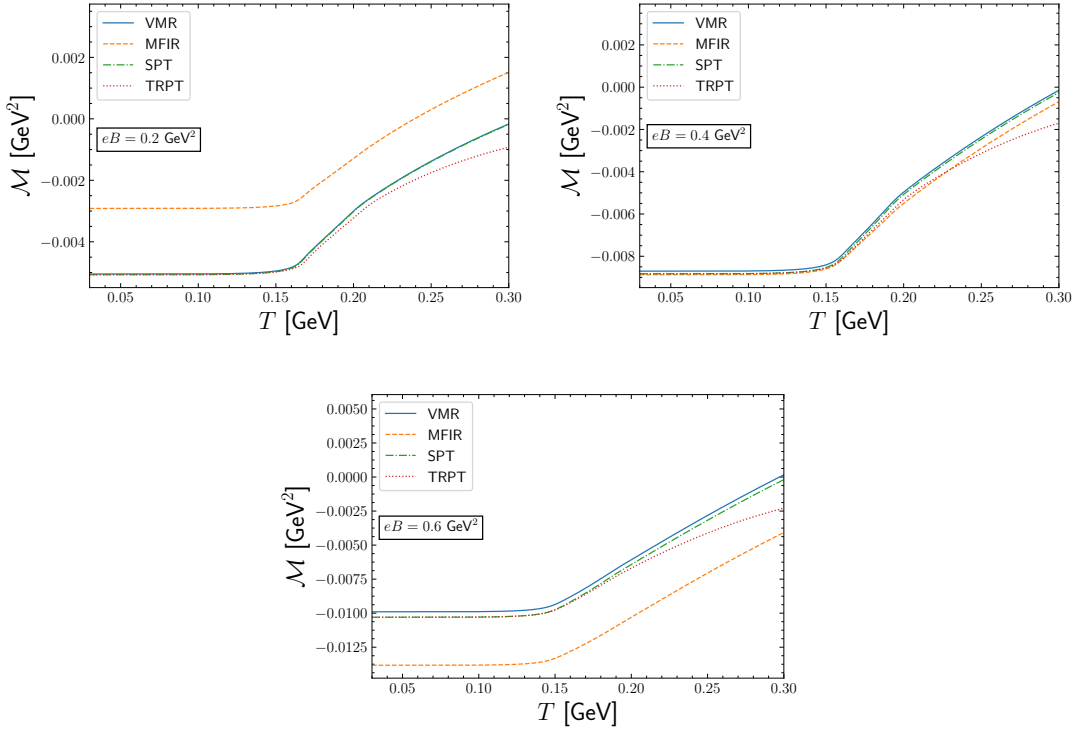


FIG. 5. Magnetization for different magnetic field values as a function of the temperature calculated with the different regularization procedures.

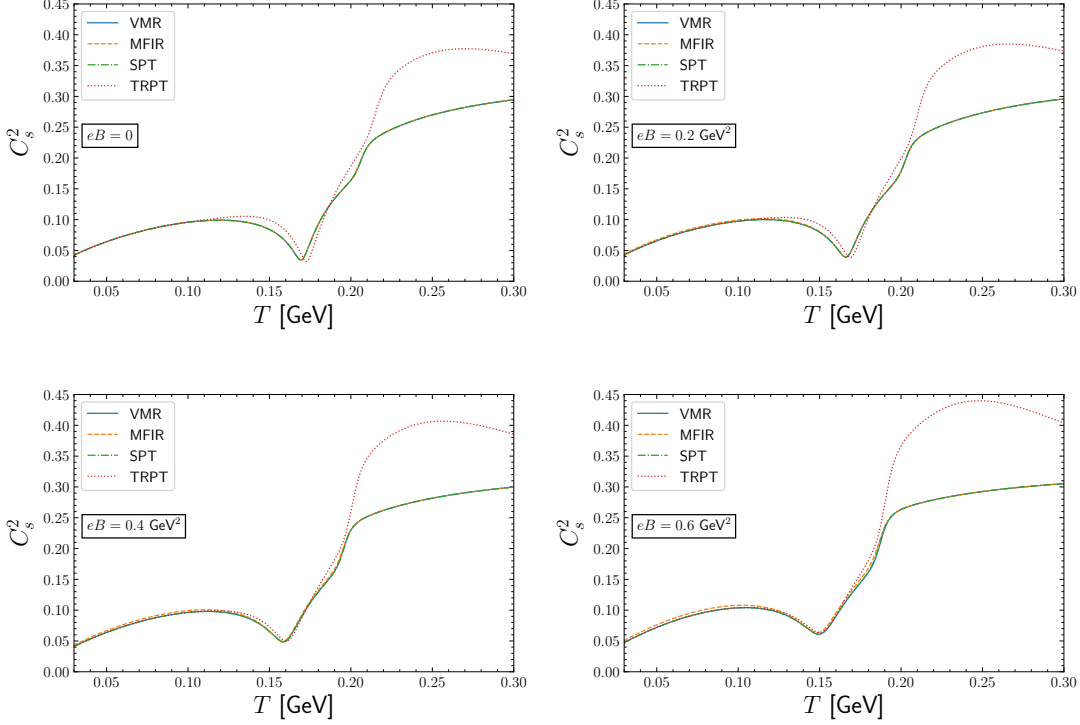


FIG. 6. The squared speed of sound for different magnetic field values as a function of temperature calculated with the different regularization procedures

predictions are in better agreement with the ones furnished by the other three prescriptions. It is also clear, from the inflection points, that the pseudocritical temperature value decreases as  $B$  increases as one could anticipate. The subtracted pressure,  $\Delta P = P(T, B) - P(0, B)$ , as a function of  $T$  is presented in Fig. 2 for different values of  $B$ . One can now observe that the TRPT scheme also produces a rather different high- $T$  behavior which is enhanced as higher magnetic fields are considered as the panel for the  $eB = 0.6 \text{ GeV}^2$  suggests. The maximum at  $T \approx 0.23 \text{ GeV}$  ( $eB = 0.6 \text{ GeV}^2$ ) is a reminder that by regulating the (convergent) thermomagnetic integrals one loses predictive power at high temperatures. As already emphasized, a major drawback of this type of regularization procedure is that the Stefan-Boltzmann limit is never attained as  $T \rightarrow \infty$  [39]. Next, to illustrate both the effect of the missing mass independent terms in the MFIR as well as the effect of regulating the thermomagnetic integrals within the TRPT schemes we offer Fig. 3. This figure shows that the TRPT predictions become less reliable as  $T$  increases, in accordance with our previous discussion. Moreover, the figure clearly illustrates how the neglected mass independent terms seem to affect the pressure by causing its absolute value to first decrease (at low  $B$ ) and then increase after having reached an extremum. This behavior is in contradiction with the ones predicted by all the other three schemes and directly affects the magnetization as Fig. 4 shows. From the qualitative point of view is important to note that the MFIR predicts quark matter to be paramagnetic ( $\mathcal{M} > 0$ ) at low  $B$  and diamagnetic ( $\mathcal{M} < 0$ ) at high magnetic fields while the other approximations predict it to be diamagnetic (at least up to the highest temperature considered in the figure,  $T = 0.25 \text{ GeV}$ ). The magnetization thermal behavior can be better analyzed by plotting this quantity as a function of  $T$  for different values of  $B$  as Fig. 5 shows. One can observe that the thermal behavior predicted by the MFIR is very sensitive to variations of  $B$ . At  $eB = 0.2 \text{ GeV}^2$  the predicted MFIR absolute value for  $\mathcal{M}$  is lesser than the ones predicted by the other approximations. Then, all the predicted values almost coincide at  $eB = 0.4 \text{ GeV}^2$  while the MFIR absolute values are higher at  $eB = 0.6 \text{ GeV}^2$ . Another interesting feature displayed in Fig. 5 concerns the high- $T$  behavior of the TRPT curves which increase with  $T$  in a less linear fashion than all other curves as one could anticipate based on our previous discussion related to the Stefan-Boltzmann limit. This problem becomes even more transparent when one analyzes the speed of sound squared as a function of the temperature. In this case Fig. 6 clearly reveals that for  $T \gtrsim 0.2 \text{ GeV}$  the TRPT scheme predicts that  $C_s^2$  overshoots the value  $1/3$  which is the expected value at the Stefan-Boltzmann limit. The other three methods, on the other hand, predict a steady convergence towards  $C_s^2 = 1/3$  as  $T \rightarrow \infty$ . Finally, Fig. 7 which shows the specific heat as a function of  $T$  for different values of  $B$  displays a clear difference between the deconfinement (first peak) and

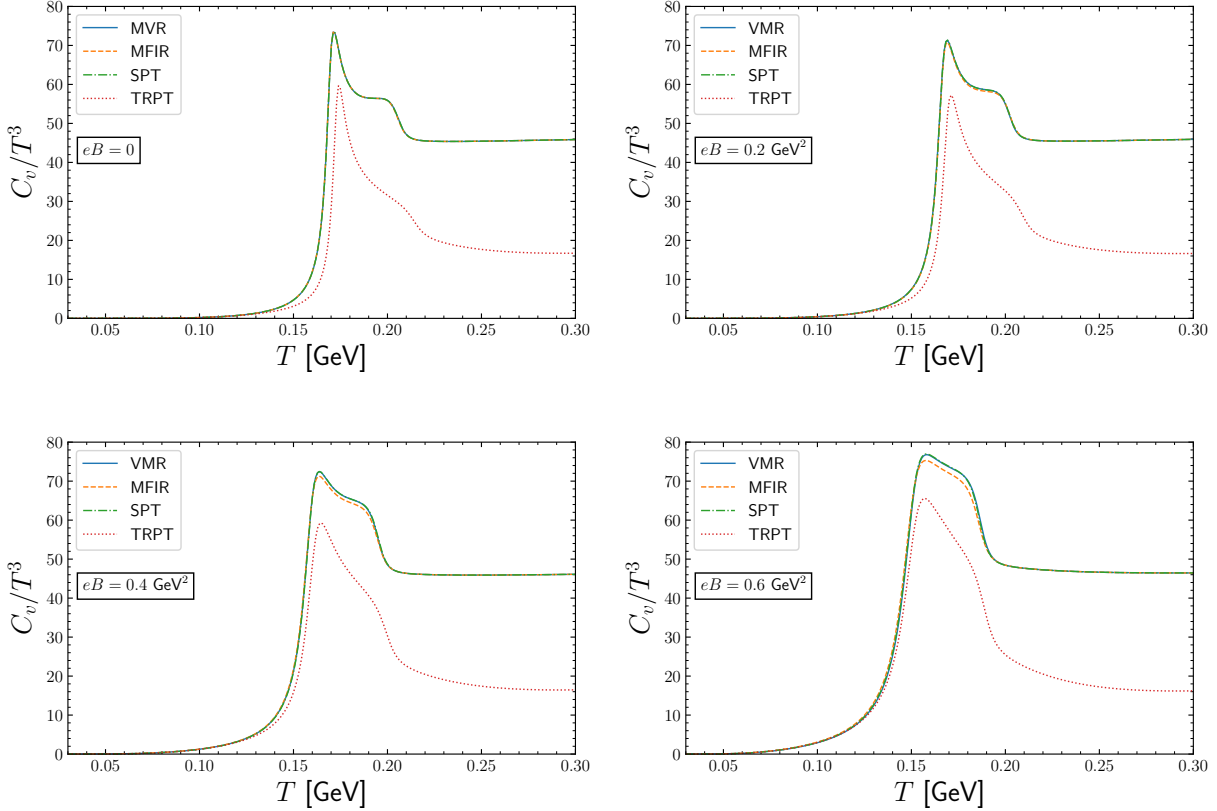


FIG. 7. The specific heat for different magnetic field values as a function of temperature calculated with the different regularization procedures.

the chiral (second peak) crossover taking place within the  $T \sim 0.15 - 0.2$ , GeV range. One observes a rather good agreement between the full MFIR, VMR and SPT prescriptions even when the magnetic field reaches high values. On the other hand, the TRPT prescription predicts much lower values when compared to the other regularization schemes especially for temperatures around and above the deconfinement pseudocritical transition. This appears to be yet another consequence of regulating the convergent thermomagnetic integrals within this model (a byproduct of underestimating the Stefan-Boltzmann limit in the pressure). For all regularization prescriptions adopted in this work one can observe the presence of two peaks in the specific heat as a function of the temperature: the first one (more abrupt) determines the pseudo critical temperature for deconfinement and the second (smoother) determines the pseudo critical temperature for chiral symmetry restoration. It is important to note that all of our results include IMC through  $G(eB)$  in the deconfinement and chiral transitions and the splitting between these pseudo critical temperatures remains almost constant if we increase the strength of the magnetic field as already reported in the context of the SU(3) PNJL [59]. This is in the opposite behavior when compared with results of SU(3) PNJL and SU(2) LSM [60, 61], where the splitting increases with  $B$ . The LQCD study [62] gives further support to the behavior found in Ref. [59].

## V. CONCLUSIONS

We have considered the two-flavor PNJL model in the presence of a thermomagnetic background within the mean field framework in order to compare four different regularization prescriptions. In non renormalizable theories the adoption of different regularization schemes may lead to rather different predictions when a magnetic field and thermal bath are present since one lacks further constraints such as the ones available to renormalizable theories (e.g., renormalization group equations). Apart from considering the three popular schemes represented by the SPT, TRPT, and MFIR we have proposed an alternative procedure (dubbed VMR). Within this scheme all divergences are first disentangled and then regulated without any further subtractions while the finite thermomagnetic contribution is

integrated over the full momentum range. Comparing the behavior of different physical observables we are able to concluded that, as expected, the TRPT fails to converge to the Stefan-Boltzmann limit when high temperatures are considered. The other three prescriptions predict similar behaviors for the quark condensate, normalized pressure, speed of sound, and specific heat. Nevertheless, the MFIR displays a rather different behavior with regard to the absolute pressure and magnetization. In particular the MFIR predictions for the latter quantity are in qualitative disagreement with the other three methods. Namely, while the SPT, TRPT and VMR predict quark matter to be diamagnetic at the  $T, B$  range analyzed here the MFIR predicts it to be paramagnetic at low  $B$  and diamagnetic at high field values. We believe that this different behavior is due to the missing field dependent terms subtracted during the MFIR renormalization process. On the other hand the results furnished by the SPT and the VMR, proposed here, are very similar both qualitatively and quantitatively. The small differences between both schemes only become apparent when examining the results for the magnetization at high field values. This probably happens because within the VMR the divergence contained in the vacuum and in the purely magnetic part have been properly isolated and regulated allowing for the sum over LL to be performed in a closed analytical form. In the view of these results one may conclude that the VMR offers the most versatile regularization scheme to describe most observables related to magnetized quark matter.

#### ACKNOWLEDGMENTS

We are grateful to Konstantin Klimenko, Pedro Costa, João Moreira and Norberto Scoccola for related discussions. This work is partially supported by Conselho Nacional de Desenvolvimento Científico e Tecnológico (CNPq), Grants No. 304758/2017-5 (R. L. S. F), No. 304518/2019-0 (S.S.A.) and No. 303846/2017-8 (M.B.P); Coordenação de Aperfeiçoamento de Pessoal de Nível Superior - (CAPES-Brazil) - Finance Code 001 (T.E.R and W.R.T); Fundação de Amparo à Pesquisa do Estado do Rio Grande do Sul (FAPERGS), Grants Nos. 19/2551- 0000690-0 and 19/2551-0001948-3 (R. L. S. F.). The work is also part of the project Instituto Nacional de Ciência e Tecnologia - Física Nuclear e Aplicações (INCT -FNA) Grant No. 464898/2014-5. T.E.R. acknowledges Conselho Nacional de Desenvolvimento Científico e Tecnológico (CNPq-Brazil) and Coordenação de Aperfeiçoamento de Pessoal de Nível Superior (CAPES-Brazil) for PhD grants at different periods of time as well as the support and hospitality of CFisUC where part of this work was developed.

### Appendix A: Vacuum Magnetic Regularization

Let us consider the (entangled) vacuum-magnetic parts of the thermodynamical potential as it appears in the lhs of Eq.(3.5)

$$I = \sum_{f=u,d} \frac{N_c}{8\pi^2} \int_{\frac{1}{\Lambda^2}}^{\infty} ds \frac{e^{-M^2 s}}{s^3} (|q_f B| s \coth(|q_f B| s)), \quad (\text{A1})$$

where, we have used a simple change of variables. Note that the integrand is clearly divergent for  $s \rightarrow 0$ . Within the VMR we first separate the integrand of Eq.(A1) into a divergent and a finite part [30] as  $s \rightarrow 0$ . With this aim, let us first expand the  $\coth(|q_f B| s)$  in Taylor series, such that

$$\frac{e^{-M^2 s}}{s^3} (|q_f B| s \coth(|q_f B| s)) = \frac{e^{-M^2 s}}{s^3} \left( 1 + \frac{(|q_f B| s)^2}{3} - \frac{(|q_f B| s)^4}{45} + O((|q_f B| s)^5) \right), \quad (|q_f B| s) < \pi. \quad (\text{A2})$$

As we can see, the first two terms in Eq.(A2) are divergent for  $s \rightarrow 0$  and need regularization so we can rewrite  $I$  as

$$I = I_0 + I_{field} + I_{int}, \quad (\text{A3})$$

where

$$I_0 = \frac{N_f N_c}{8\pi^2} \int_{\frac{1}{\Lambda^2}}^{\infty} ds \frac{e^{-M^2 s}}{s^3}, \quad (\text{A4})$$

$$I_{field} = \sum_{f=u,d} \frac{N_c}{3} \frac{(|q_f B|)^2}{8\pi^2} \int_{\frac{1}{\Lambda^2}}^{\infty} ds \frac{e^{-M^2 s}}{s}, \quad (\text{A5})$$

and the finite pure magnetic contribution  $I_{int}$  is

$$I_{int} = \sum_{f=u,d} \frac{N_c}{8\pi^2} \int_0^{\infty} ds \frac{e^{-M^2 s}}{s^3} \left( |q_f B| s \coth(|q_f B| s) - 1 - \frac{(|q_f B| s)^2}{3} \right). \quad (\text{A6})$$

Now, we can solve the finite integral (A6) using the representation of the gamma function,

$$\frac{\Gamma(n+1)}{(\beta)^{n+1}} = \int_0^{\infty} ds s^n e^{-\beta s}, \quad (\text{A7})$$

and the Hurwitz-Rieman-zeta function [63],

$$\zeta(z, q) = \sum_{k=0}^{\infty} \frac{1}{(q+k)^z}, \quad (\text{A8})$$

such that

$$\begin{aligned} I_{int} &= \sum_{f=u,d} N_c \lim_{\epsilon \rightarrow 0} \frac{(|q_f B|)^2}{8\pi^2} \int_0^{\infty} ds e^{-\frac{M^2}{|q_f B|} s} s^{-3+\epsilon} \left( s \coth(s) - 1 - \frac{s^2}{3} \right) \\ &= \sum_{f=u,d} N_c \frac{(|q_f B|)^2}{8\pi^2} \lim_{\epsilon \rightarrow 0} \left[ \Gamma(-1+\epsilon) \left( 2^{2-\epsilon} \zeta(-1+\epsilon, \frac{M^2}{2|q_f B|}) - \left( \frac{M^2}{|q_f B|} \right)^{1-\epsilon} \right) - \frac{\Gamma(-2+\epsilon)}{\left( \frac{M^2}{|q_f B|} \right)^{-2+\epsilon}} - \frac{1}{3} \frac{\Gamma(\epsilon)}{\left( \frac{M^2}{|q_f B|} \right)^\epsilon} \right]. \end{aligned} \quad (\text{A9})$$

Making use of some expansions such as  $a^{-\epsilon} \cong 1 - \ln a \epsilon + O(\epsilon)$ , and

$$\Gamma(-n+\epsilon) = \frac{(-1)^n}{n!} \left[ \frac{1}{\epsilon} + \psi_1(n+1) + O(\epsilon) \right], \quad (\text{A10})$$

where  $\psi_1(n+1) = 1 + \frac{1}{2} + \dots + \frac{1}{n} - \gamma_E$ , and  $\gamma_E = 0.577216$  is the Euler-Mascheroni constant. After some algebraic steps we then obtain

$$I_{int}(B) = -N_c \sum_{f=u,d} \frac{|q_f B|^2}{2\pi^2} \left[ \zeta'(-1, x_f) - \frac{1}{2}(x_f^2 - x_f) \ln x_f + \frac{x_f^2}{4} - \frac{1}{12}(1 + \ln x_f) \right], \quad (\text{A11})$$

where we have defined  $x_f = M^2/(2|q_f B|)$  so that Eq. (A3) is exactly the rhs of Eq. (3.5). The main difference between this VMR scheme and the MFIR [44] is that within the latter the (magnetic) divergent term represented by  $I_{field}$ , given by Eq. (A5), is completely subtracted by a field renormalization. In this process  $B$ -dependent finite terms, such as the ones proportional to  $(1 + \ln x)/12$  in Eq. (A11), are also subtracted (see Ref. [44] for further details) leading to the two different thermodynamical potentials considered in Sec. III.

---

[1] R. C. Duncan and C. Thompson, *Astrophys. J. Lett.* **392**, L9 (1992).

[2] K. Fukushima, D. E. Kharzeev, and H. J. Warringa, *Phys. Rev. D* **78**, 074033 (2008), arXiv:0808.3382 [hep-ph].

[3] D. E. Kharzeev and H. J. Warringa, *Phys. Rev. D* **80**, 034028 (2009), arXiv:0907.5007 [hep-ph].

[4] D. E. Kharzeev, *Nucl. Phys. A* **830**, 543C (2009), arXiv:0908.0314 [hep-ph].

[5] G. Bali, F. Bruckmann, G. Endrodi, Z. Fodor, S. Katz, and A. Schafer, *Phys. Rev. D* **86**, 071502 (2012), arXiv:1206.4205 [hep-lat].

[6] A. Bandyopadhyay and R. L. Farias, (2020), arXiv:2003.11054 [hep-ph].

[7] M. D'Elia, S. Mukherjee, and F. Sanfilippo, *Phys. Rev. D* **82**, 051501 (2010), arXiv:1005.5365 [hep-lat].

[8] M. D'Elia and F. Negro, *Phys. Rev. D* **83**, 114028 (2011), arXiv:1103.2080 [hep-lat].

[9] E.-M. Ilgenfritz, M. Kalinowski, M. Muller-Preussker, B. Petersson, and A. Schreiber, *Phys. Rev. D* **85**, 114504 (2012), arXiv:1203.3360 [hep-lat].

[10] G. Endrődi, M. Giordano, S. D. Katz, T. Kovács, and F. Pittler, *JHEP* **07**, 007 (2019), arXiv:1904.10296 [hep-lat].

[11] Y. Nambu and G. Jona-Lasinio, *Phys. Rev.* **122**, 345 (1961); *Phys. Rev.* **124**, 246 (1961).

[12] O. Scavenius, A. Mocsy, I. Mishustin, and D. Rischke, *Phys. Rev. C* **64**, 045202 (2001), arXiv:nucl-th/0007030.

[13] E. S. Fraga and A. J. Mizher, *Phys. Rev. D* **78**, 025016 (2008), arXiv:0804.1452 [hep-ph].

[14] C. Ratti, M. A. Thaler, and W. Weise, *Phys. Rev. D* **73**, 014019 (2006), arXiv:hep-ph/0506234.

[15] B.-J. Schaefer, M. Wagner, and J. Wambach, *Phys. Rev. D* **81**, 074013 (2010), arXiv:0910.5628 [hep-ph].

[16] K. Fukushima and Y. Hidaka, *Phys. Rev. Lett.* **110**, 031601 (2013), arXiv:1209.1319 [hep-ph].

[17] R. Farias, K. Gomes, G. Krein, and M. Pinto, *Phys. Rev. C* **90**, 025203 (2014), arXiv:1404.3931 [hep-ph].

[18] E. Ferrer, V. de la Incera, and X. Wen, *Phys. Rev. D* **91**, 054006 (2015), arXiv:1407.3503 [nucl-th].

[19] A. Ayala, C. Dominguez, S. Hernández-Ortiz, L. Hernández, M. Loewe, D. Manreza Paret, and R. Zamora, *Phys. Rev. D* **98**, 031501 (2018), arXiv:1805.08198 [hep-ph].

[20] A. Ayala, L. Hernández, M. Loewe, A. Raya, J. Rojas, and R. Zamora, *Phys. Rev. D* **96**, 034007 (2017), arXiv:1706.04956 [hep-ph].

[21] A. Ayala, C. Dominguez, L. Hernández, M. Loewe, A. Raya, J. Rojas, and C. Villavicencio, *Phys. Rev. D* **94**, 054019 (2016), arXiv:1603.00833 [hep-ph].

[22] A. Ayala, C. Dominguez, L. Hernández, M. Loewe, and R. Zamora, *Phys. Lett. B* **759**, 99 (2016), arXiv:1510.09134 [hep-ph].

[23] A. Ayala, C. Dominguez, L. Hernández, M. Loewe, and R. Zamora, *Phys. Rev. D* **92**, 096011 (2015), [Addendum: *Phys. Rev. D* 92, 119905 (2015)], arXiv:1509.03345 [hep-ph].

[24] R. Farias, V. Timóteo, S. Avancini, M. Pinto, and G. Krein, *Eur. Phys. J. A* **53**, 101 (2017), arXiv:1603.03847 [hep-ph].

[25] G. Endrődi and G. Markó, *JHEP* **08**, 036 (2019), arXiv:1905.02103 [hep-lat].

[26] M. Ferreira, P. Costa, O. Lourenço, T. Frederico, and C. Providência, *Phys. Rev. D* **89**, 116011 (2014), arXiv:1404.5577 [hep-ph].

[27] M. Ferreira, P. Costa, D. P. Menezes, C. Providência, and N. Scoccola, *Phys. Rev. D* **89**, 016002 (2014), [Addendum: *Phys. Rev. D* 89, 019902 (2014)], arXiv:1305.4751 [hep-ph].

[28] J. Moreira, P. Costa, and T. E. Restrepo, *Phys. Rev. D* **102**, 014032 (2020), arXiv:2005.07049 [hep-ph].

[29] J. O. Andersen, W. R. Naylor, and A. Tranberg, *Rev. Mod. Phys.* **88**, 025001 (2016), arXiv:1411.7176 [hep-ph].

[30] J. S. Schwinger, *Phys. Rev.* **82**, 664 (1951).

[31] P. Costa, H. Hansen, M. Ruivo, and C. de Sousa, *Phys. Rev. D* **81**, 016007 (2010), arXiv:0909.5124 [hep-ph].

[32] M. Ruivo, P. Costa, H. Hansen, and C. de Sousa, *AIP Conf. Proc.* **1257**, 681 (2010), arXiv:1001.3077 [hep-ph].

[33] P. Costa, M. Ruivo, C. de Sousa, and H. Hansen, *Symmetry* **2**, 1338 (2010), arXiv:1007.1380 [hep-ph].

[34] S. Fayazbakhsh, S. Sadeghian, and N. Sadooghi, *Phys. Rev. D* **86**, 085042 (2012), arXiv:1206.6051 [hep-ph].

[35] S. S. Avancini, R. L. Farias, N. N. Scoccola, and W. R. Tavares, *Phys. Rev. D* **99**, 116002 (2019), arXiv:1904.02730 [hep-ph].

[36] P. G. Allen, A. G. Grunfeld, and N. N. Scoccola, *Phys. Rev. D* **92**, 074041 (2015), arXiv:1508.04724 [hep-ph].

[37] T. Inagaki, D. Kimura, H. Kohyama, and A. Kvinikhidze, *Phys. Rev. D* **86**, 116013 (2012), arXiv:1202.5220 [hep-ph].

[38] M. Buballa, *Physics Reports* **407**, 205–376 (2005).

[39] P. Zhuang, J. Hufner, and S. Klevansky, *Nucl. Phys. A* **576**, 525 (1994).

[40] K. Fukushima, *Phys. Lett. B* **591**, 277 (2004), arXiv:hep-ph/0310121.

[41] N. M. Bratovic, T. Hatsuda, and W. Weise, *Phys. Lett. B* **719**, 131 (2013), arXiv:1204.3788 [hep-ph].

[42] J. Moreira, B. Hiller, A. Osipov, and A. Blin, *Int. J. Mod. Phys. A* **27**, 1250060 (2012), arXiv:1008.0569 [hep-ph].

[43] S. Klevansky and R. H. Lemmer, *Phys. Rev. D* **39**, 3478 (1989).

[44] D. Ebert and K. Klimenko, *Nucl. Phys. A* **728**, 203 (2003), arXiv:hep-ph/0305149.

[45] D. Ebert, K. Klimenko, M. Vdovichenko, and A. Vshivtsev, *Phys. Rev. D* **61**, 025005 (2000), arXiv:hep-ph/9905253.

[46] D. Menezes, M. Benghi Pinto, S. Avancini, A. Perez Martinez, and C. Providência, *Phys. Rev. C* **79**, 035807 (2009), arXiv:0811.3361 [nucl-th].

[47] S. S. Avancini, D. P. Menezes, M. B. Pinto, and C. Providência, *Phys. Rev. D* **85**, 091901 (2012), arXiv:1202.5641 [hep-ph].

[48] D. Menezes, M. Benghi Pinto, S. Avancini, and C. Providência, *Phys. Rev. C* **80**, 065805 (2009), arXiv:0907.2607 [nucl-th].

[49] S. S. Avancini, R. L. S. Farias, M. Benghi Pinto, W. R. Tavares, and V. S. Timóteo, *Phys. Lett. B* **767**, 247 (2017), arXiv:1606.05754 [hep-ph].

[50] S. S. Avancini, V. Dexheimer, R. L. S. Farias, and V. S. Timóteo, *Phys. Rev. C* **97**, 035207 (2018), arXiv:1709.02774 [hep-ph].

[51] S. S. Avancini, R. L. Farias, and W. R. Tavares, *Phys. Rev. D* **99**, 056009 (2019), arXiv:1812.00945 [hep-ph].

[52] M. Coppola, P. Allen, A. Grunfeld, and N. Scoccola, *Phys. Rev. D* **96**, 056013 (2017), arXiv:1707.03795 [hep-ph].

[53] D. C. Duarte, P. Allen, R. Farias, P. H. A. Manso, R. O. Ramos, and N. Scoccola, *Phys. Rev. D* **93**, 025017 (2016), arXiv:1510.02756 [hep-ph].

[54] D. C. Duarte, R. Farias, P. H. Manso, and R. O. Ramos, *J. Phys. Conf. Ser.* **706**, 052010 (2016).

[55] G. Endrődi, *JHEP* **04**, 023 (2013), arXiv:1301.1307 [hep-ph].

[56] K. Fukushima and C. Sasaki, *Prog. Part. Nucl. Phys.* **72**, 99 (2013), arXiv:1301.6377 [hep-ph].

[57] C. Ratti, S. Roessner, M. Thaler, and W. Weise, *Eur. Phys. J. C* **49**, 213 (2007), arXiv:hep-ph/0609218.

[58] B.-J. Schaefer, J. M. Pawłowski, and J. Wambach, *Phys. Rev. D* **76**, 074023 (2007), arXiv:0704.3234 [hep-ph].

[59] M. Ferreira, P. Costa, and C. Providência, *Phys. Rev. D* **90**, 016012 (2014), arXiv:1406.3608 [hep-ph].

[60] M. Ferreira, P. Costa, and C. Providência, *Phys. Rev. D* **89**, 036006 (2014), arXiv:1312.6733 [hep-ph].

[61] A. J. Mizher, M. Chernodub, and E. S. Fraga, *Phys. Rev. D* **82**, 105016 (2010), arXiv:1004.2712 [hep-ph].

[62] G. Bali, F. Bruckmann, G. Endrődi, Z. Fodor, S. Katz, S. Krieg, A. Schafer, and K. Szabo, *JHEP* **02**, 044 (2012), arXiv:1111.4956 [hep-lat].

[63] I. S. Gradshteyn and I. M. Ryzhik, *Table of integrals, series, and products*, seventh ed. (Elsevier/Academic Press, Amsterdam, 2007).